The relation between well spacing and Net Present Value in fluvial Hot Sedimentary Aquifer geothermal doublets

a West Netherlands Basin case study

Willems, Cees; Goense, Twan; Maghami Nick, Hamid; Bruhn, David

Publication date
2016

Document Version
Final published version

Published in
Proceedings of the 41st Workshop on Geothermal Reservoir Engineering

PROCEEDINGS, 41st Workshop on Geothermal Reservoir Engineering
Stanford University, Stanford, California, February 22-24, 2016
SGP-TR-209

The relation between well spacing and Net Present Value in fluvial Hot Sedimentary Aquifer geothermal doublets; a West Netherlands Basin case study

C.J.L. Willems; T. Goense; H.M. Nick; D.F. Bruhn

c.j.l.willems@tudelft.nl

Keywords: Hot Sedimentary Aquifers, Net Present Value, West Netherlands Basin, Direct Use, Reservoir Engineering

ABSTRACT

This paper analyzes the relation between well spacing and Net Present Value of a Hot Sedimentary Aquifer geothermal doublet. First, a sensitivity analysis is carried out to evaluate the effect of uncertainty of geological and production parameters on the Net present Value. Second a finite-element approach is utilized to study the effect of fluvial facies architecture on geothermal energy production. For this purpose detailed fluvial facies architecture models are created utilizing a process-based facies modelling approach. These models and reservoir properties are based on a geological dataset of the Lower Cretaceous Nieuwerkerk Formation in the West Netherlands Basin (WNB). Results of the sensitivity analysis show that a 10% variation in well spacing from a 1000m base case scenario could vary the NPV by 10%. The minimal required well spacing is dependent on the reservoir thickness, flow rate and the allowed production temperature drop. The simulations results show that the theoretical advantage of a reduction in well spacing could be balanced by a poor well connectivity between the wells because of the characteristic of fluvial reservoir architecture.

1. INTRODUCTION

Large potential resources of heat are stored in sedimentary rocks (Boxem et al., 2011). Currently geothermal energy production from Hot Sedimentary Aquifers (HSA) is only developed in a limited number of regions. Examples of sedimentary basins with geothermal energy exploitation are the Paris Basin (Lopez et al. 2010), the Perth Basin Australia (Pujol et al., 2015) and the West Netherlands Basin (Van Heekeren & Bakema, 2015). Interest in sedimentary aquifers has increased and studies have been carried out to predict the potential in new regions (Deo et al., 2014). Still, the high initial investment costs, low financial gain in combination with the large geological uncertainties limit the growth of HSA geothermal development (Held et al., 2014). The geological uncertainties in sedimentary aquifers and their effect on production are extensively studied for oil and gas production (Larue & Friedmann, 2005; Larue & Hovadik, 2006; Larue & Hovadik, 2008) and to less extend for HSA geothermal exploitation (Hamm & Lopez, 2012). The assessment of these uncertainties determine the three main human controlled parameters in HSA doublets. These include the well spacing, well orientation with respect to reservoir trends and the flow rate. Together they determine doublet performance. In the West Netherlands Basin and Paris Basin, current doublets typically have a well spacing of more than 1000m to ensure sufficient doublet life-time (Mijnlieff et al., 2007; Mottaghy et al., 2011; Lopez et al., 2010). The long spacing distance could lead to unnecessary long thermal breakthrough time. Previous studies show that thermal breakthrough times of 30-50 years can be expected as a result of typical WNB flow rates of ~100-150m^3/h, ~50-150m reservoirs thickness and 1000-1500 m well spacing (Mijnlieff et al., 2007; Mottaghy et al., 2011, Saeid et al., 2015). In HSA life time predictions often two crucial factors are not taken into account. The first factor is the thermal recharge from over- and under burden which could considerably increase these life-time estimates (Poulsen et al., 2015). The second factor is the reservoir architecture or facies heterogeneities. These features increase the flow path length between wells and could provide thermal recharge, increasing the life-time. The current large well spacing design might be overcautious. A reduction of well spacing could still result in sufficient life time, while improving the financial situation of a doublet. First, it reduces the drilling costs. Second, it could reduce the required pump energy due to shorter flow paths between the wells. In addition, it decreases the chance on flow baffles between the wells such as sealed sub-seismic faults or poor sandstone body connectivity (Larue & Hovadik, 2006; Pranter & Sommer, 2011). Finally, more doublets could be realized in the same aquifer which increases the amount of produced geothermal heat (Mijnlieff et al., 2007).

The first goal of this study is to analyze the sensitivity of the NPV to various geological and production parameters. Base case values of these parameters are derived from WNB HSA doublet examples (Motthagy et al., 2011; Van Wees et al., 2012; Gonzales, 2013, Van Heekeren & Bakema, 2015). The NPV analysis is based on the NPV model from Van Wees et al. (2010). Life time estimations in this first part are based on the Gringarten et al., (1978) radial flow equation.

In the second part of this paper, finite-element production simulations are carried out to determine whether sufficient life-time can be expected, if the well spacing is reduced below 1000m. For this purpose a process-based facies modelling approach is utilized to generate detailed facies architecture reservoir models. Thirteen different models are generated with N/G values that range from 15-70%. This range in N/G and the geological model of the reservoir are based on geological well and core data from the WNB. As a result, this study will evaluate the advantages as well as the risks of smaller well spacing. This evaluation should decrease uncertainties and improve the competitiveness of HSA doublets to other energy sources.

2. WEST NETHERLANDS BASIN HSA EXPLOITATION AND GEOLOGICAL MODEL

In the WNB currently seven geothermal doublet systems are realized since 2007 (Van Heekeren & Bakema. 2015). All doublets target a Lower Cretaceous sandstone rich interval. During the Lower Cretaceous, a syn-rift meandering fluvial system formed the Nieuwerkerk Formation (DeVault & Jeremiah, 2002). The fluvial sediments are covered by an increasingly marine and lagoonal interval that is referred to as the Rodenrijs Claystone Member (Van Adrichem Boogeart & Kouwe, 1993). The geothermal doublets target lower fault blocks in the inverted WNB. Reservoir property predictions are based on subsurface well and core data from oil and gas production in the pas ~60 years. Oil and gas wells target the structural highs surrounding the lower geothermal fault blocks (TNO,1977). The available subsurface data from the currently 7 geothermal doublets is limited. Due to cost reductions, often only gamma-ray (GR) logs and surface pressure and temperature measurements are available. Six of these GR logs are presented in Figure 1. These logs show that the reservoir thickness ranges from ~50-150 m (~160-490 ft.) and the net-sandstone volume (N/G) ranges approximately from 10-70%. Based on core data the paleo flow depth is determined at ~4m (DeVault & Jeremiah, 2002). The associated paleo bank-full width is estimated at 20-40 m (66 – 131 ft.) and the sandstone body width is assumed to range between 50-400m (Gibling, 2006; Donselaar & Overeem, 2008; Pranter & Sommer, 2011). These geometry parameters are used The reservoir depth varies from 1600-3000 meter with associated temperatures between 60-90 ^{0}C (Bonté et al., 2012). Reservoir parameters for the life time and NPV calculations and input for the process-based facies modelling in this paper are derived from these WNB data.

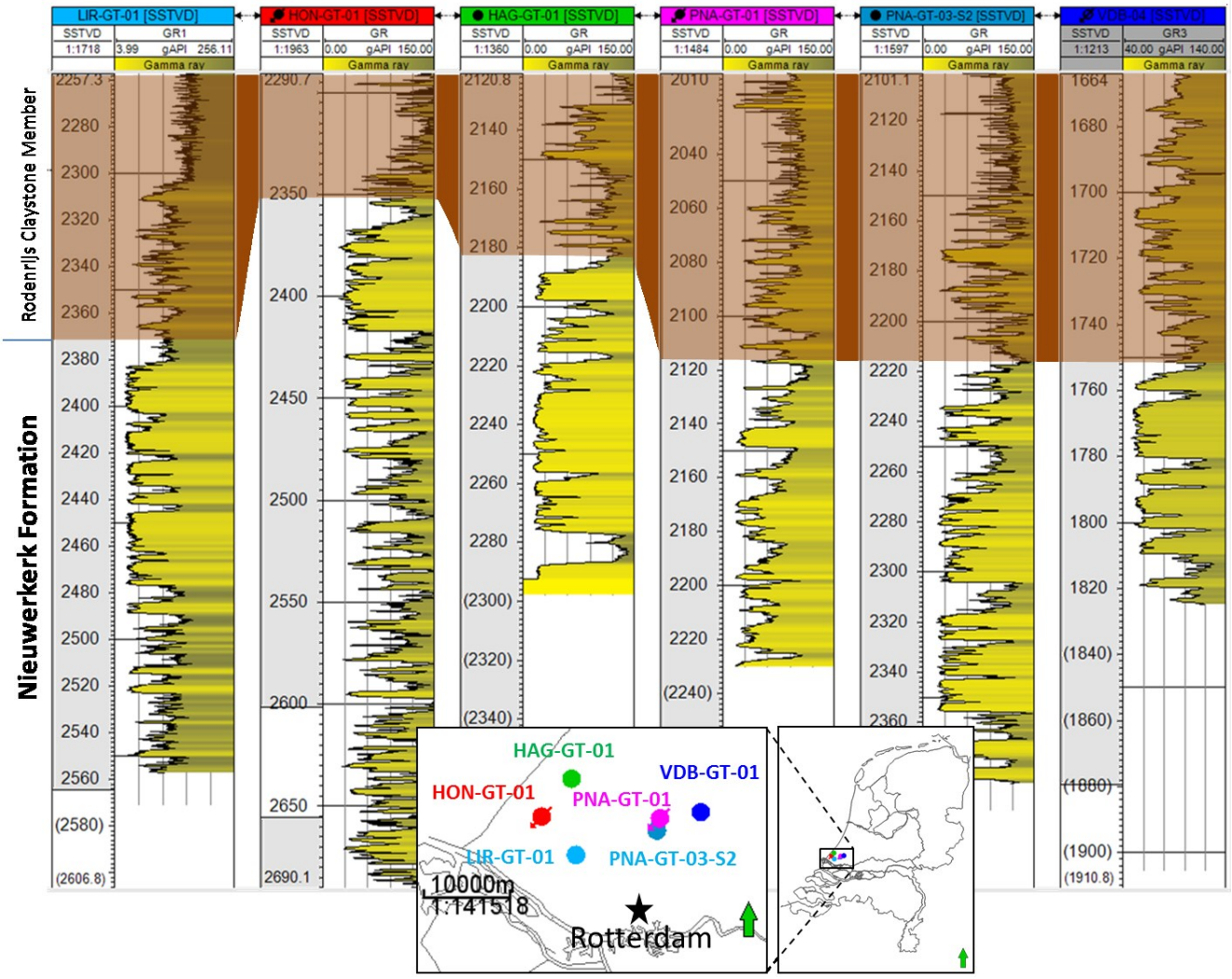

Figure 1: Gamma-ray (GR) logs from WNB geothermal doublets. Low GR readings indicate sandstone (yellow), high GR reading indicate finer grained sediments such as silt and clay. Depth is indicated in SSTVD, Standard True Vertical Depth. Locations of the corresponding well heads are presented on the map.

3. METHOD

NPV calculations of a doublet are based on estimations of heat flow and the associated pump energy losses. Pump energy losses and the production heat flow are estimated using equation 1 and 2.

$$\boldsymbol{Q_{heat} = \rho_f C_f Q \cdot \Delta T} \quad (1)$$

$$\boldsymbol{P_{Pump} = \frac{Q \cdot \Delta P}{\varepsilon}} \quad (2)$$

In equation 1, Q is the production flow rate, ΔT is the temperature difference between the production and injection water, of the production water density, C_f the production water heat capacity. Typical flow rates in WNB geothermal doublets range from 100-200 m3/h (27-55 L/s) (Van Heekeren & Bakema. 2015) and the re-injected temperature ranges commonly 30-45 °C depending on the season. In calculations in this paper, the reservoir depth is 2000m with an associated 75°temperature (section 2) . In equation 2, ΔP is the pressure difference between the doublet wells and ε the pump efficiency. Because of the large uncertainty associated with pump energy losses equation 2, the pump efficiency (ε) is varied in this analysis from 65-85%. The net-produced energy in Watt is the sum of both equations 1 and 2. For simplicity the production continues 100% of the time, Work-over, maintenance and reduced production in hotter summer months for example are neglected.

In the first part of this paper, estimations of the life time, the production temperature development and the pressure difference over the doublet wells are based on the Gringarten (1978) radial flow equation (section 3.1). In the second part of this paper the pump pressure difference between the wells and the life time are derived from finite-element production simulations. This is carried out first to determine how the fluvial reservoir architecture influences life time and second whether sufficient life-time can be expected if the well spacing is reduced below the 1000m standard. The generation of the reservoir models, property modelling and the governing equations are described in section 3.2. Two life time scenarios are considered the finite element simulations. First, the life time can be considered as the moment that the production temperature starts to decline. Assuming that heat exchangers can still produce heat after the first temperature reduction, one could also define life time as the moment after which temperature reduced by 10% of the initial reservoir temperature. The NPV model is introduced in section 3.3.

3.1 Life time and energy production estimations in part 1

Equation 3 presents the radial flow equation of Gringarten (1978):

$$\boldsymbol{t = \frac{\pi h L^2}{3Q} \frac{\rho_s C_s}{C_f \rho_f}} \quad (3)$$

In this equation the life time (t) is a function of the flow rate (Q), reservoir height (h), the doublet spacing (L), heat capacities of reservoir rock and fluid (C_f and C_s and respectively) and the density of reservoir and the production fluid (ρ_f and ρ_s and respectively). The base case scenario reservoir has a 50 meter thickness and a 40% N/G. This thickness is a conservative assumption. However it will decrease the computation time drastically in the finite-element production simulations. The required pressure difference (ΔP) in the doublet is estimated using equation (4):

$$\boldsymbol{\Delta P = \left(\frac{Q \mu}{\pi k h}\right) \ln\left(\frac{L}{r_w} - 1\right)} \quad (4)$$

The water viscosity (μ) is estimated to be 0.001 Pa.s, the average reservoir permeability (k) 1000 mD (TNO,1977), and the wellbore radius (r_w) is 0.1 m.

3.2 Finite-element production simulations

In the second part of this paper, production temperature and required production and injection pressure are generated in finite-element production simulations. The reservoir models in these simulations consist of three layers, each of 1km x 2km x 50m. The reservoir layer is confined between two impermeable shale over- and underburden layers, providing thermal recharge (Poulsen et al., 2015). One production well and an injection well with a well spacing L are placed in the reservoir layer. The modelling of the reservoir properties is based on a process-based facies modelling approach (Cojan et al., 2004, Grappe et al. (2012). For this purpose, geological parameters are derived from WNB subsurface data, which are described in section 2. Section 3.2.1 describes the facies modelling in more detail. The models contain reservoir sandstone grid blocks and impermeable claystone grid blocks. In the models, the net-to-gross (N/G), or in other words net sandstone volume is varied. Two of them have a N/G of 15%, three have a 25% N/G, three 32.5% N/G , three 45% N/G, one 60% N/G and one 70% N/G. In each facies model, four different well spacing distances (L) are considered. They include 400, 600, 800 and 1000m. A requirement of the well locations is that both wells intersect an equal amount of sandstone. In addition three production flow rates are compared. These include 100, 150 and 200 m^3/h. In total, hundred-fifty-six production simulations are required. The results are compared to production simulations in homogeneous reservoir models. The thickness in these homogeneous models is adjusted with the same N/G range. In this way, the homogeneous models have a similar range in net sandstone volume. In section 3.2.2 the distribution of permeability and porosity is explained. Finally, section 3.2.3 describes the governing equations for reservoir flow and heat transport, boundary conditions, assumptions and hydraulic and thermal parameters.

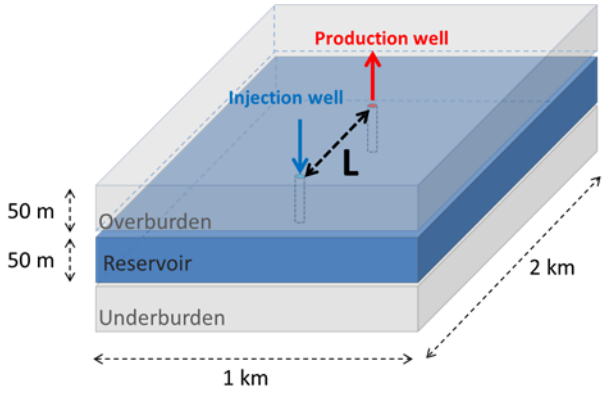

Figure 2: A reservoir layer with detailed process-based facies modeling is over- and underlain by impermeable shale layers. An injection and production well are placed with a well spacing distance L.

3.2.1 Process-based facies modelling of the reservoir layer

Rectangular 1kmx2kmx50m reservoir facies models are generated using process-based facies modelling software Flumy (Cojan et al., 2004, Lopez et al., 2009; Grappe et al., 2012). The model dimensions relate to a typical area of influence of HSA geothermal doublets (e.g. Lopez et al., 2010). The grid blocks have dimensions of 20mx20mx5m. This resolution is chosen because grid block width should be smaller than the minimal sandstone body width and height. Input parameters of the process-based approach describe sedimentological processes such as avulsion frequency, flood frequency, paleo-channel width and depth, maximum floodplain deposit thickness and topography of the floodplain. Seven types of geobodies are distributed; pointbars, sand plugs, channel lag, crevasse splays (tree types), overbank floodplain fines. Different sedimentary processes form low and high N/G reservoirs respectively which have different sandstone body geometries and architecture. The method is explained in detail in Cojan et al., 2004, Grappe et al. (2012) and Lopez et al. (2009). By varying the process parameters, models in our study have a wide range of net-to-gross (15-70%), reservoir architecture and sandstone body dimensions. The ranges of process parameter values that are used for the modelling are presented and discussed in Table 1. Ranges of values are utilized to take the uncertainties in the sedimentary input parameters of the process-based approach into account. Because only 1D subsurface data is available, the process-based approach is assumed to be an attractive facies modelling method compared to more conventional object-based approach (Villamizar et al., 2015). Estimations of the type of depositional environment, bank-full flow width can be made with more certainty compared to estimations on width and spatial relation of sediment bodies. In fact, these are dependent on many more parameters (Bridge, 2006; Gibling, 2006, Flood & Hampson, 2015). In the process-based approach however, these 3D parameters are a result of the 1D input. In facies models, the paleo flow direction is parallel to the long edge.

Table 1: A list of the varying process parameters applied in Flumy and their effect on facies distribution. The ranges of values used in this project are presented on the right side of the table.

River cross-section with process-parameters:

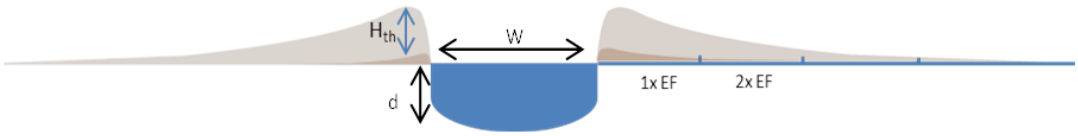

Parameter:	Consequence:	value/range
Avulsion frequency	1. Affect aggradation of the floodplain. 2. Affect sinuosity. 3. Vertical sandstone proportion	500-1000 years
Maximum overbank flood thickness (Hth)	High OB intensity favors aggradation, shale, and vertical connectivity of sand.	0,2-0.6m (0.66 - 2.0 ft.)
Floodplain deposit thickness decrease (EF)	EF influences topography of the floodplain deposit.	300-600m (980-2000 ft.)

High EF:

Low EF:

Flood (OB) frequency	Frequent OB's favor aggradation, shale deposition.	50 – 120 years

3D example of facies model:

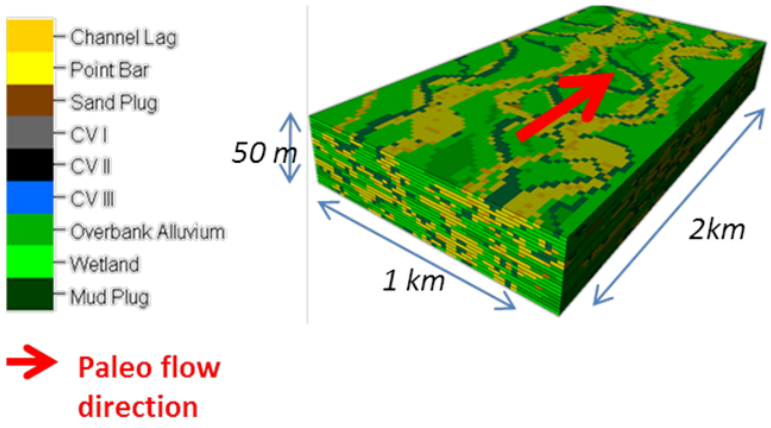

3.2.2 Property modeling of the reservoir layer

The facies bodies that result from the process-based modelling are divided into two classes, reservoir and non-reservoir. Non reservoir facies include crevasse splays, levees, overbank alluvium and mud plugs. These bodies are all assumed to be impermeable and homogeneous. Their assumed permeability is 5 mD and porosity 10%. Pointbars, sand plugs and channel lag bodies are all assumed to be reservoir grid blocks. A beta distribution correlation function was used to generate a heterogeneous porosity field within the sand group based on WNB core plug measurements (TNO,1077). The distribution characteristics including: mean, standard deviation, skew and kurtosis are equal to 0.28, 0.075, 0.35 and 2.3, respectively. Also the permeability of the reservoir grid blocks is derived from petrophysical data of well MKP-11 (TNO, 1977). From core plug measurements a porosity-permeability relationship obtained equal to $k = 0.0633\ e^{29{,}507 \cdot \varphi}$. In this equation, k is the permeability [mD] and φ is the porosity [-]. In reality sandstone grain size heterogeneity within sandstone bodies depends on paleo flow speed, and the proximity to the channel axis and river bends. As a result, the permeability of channel lags, point-bars and sand plugs varies across sandstone bodies (Willis and Tang, 2010) which could influence connectivity (Hovadik & Larue, 2008). Small scale sedimentary heterogeneities can affect permeability anisotropy within the sandstone bodies. Examples of such heterogeneities are shale drapes, accretion surfaces and bedding planes. These features decrease on average the permeability perpendicular to the paleo flow direction. This can be accounted for adjusting the permeability in different direction in each grid block like in Bierkens & Weerts (1994). To focus on facies architecture connectivity as Ainsworth et al., 2005 describe, this anisotropy in permeability is neglected. Small scale heterogeneities are assumed to be captured by using the sandstone permeability distribution from core measurements of the Lower Cretaceous Nieuwerkerk Formation core measurements. After the classification of facies in reservoir and non-reservoir, facies models are henceforth referred to as reservoir models.

3.2.3 Governing equations

In the finite-element production simulations the energy balance is solved for a rigid medium fully saturated with water, in which thermal equilibrium is assumed between the fluid and solid phases (equation 5).

$$\rho C \frac{\partial}{\partial t} T + \rho_w C_w \nabla \cdot (\mathrm{q\ T}) - \nabla \lambda \cdot (\nabla T) = 0; \tag{5}$$

In this balance, t (s) is time, T (K) is the temperature, φ is the porosity, ρ is the mass density (kg/m^3), C (J/kgK) is the specific heat capacity, λ (W/mK) is the thermal conductivity, and q (m/s) is the Darcy velocity. The suffix w refers to the pore fluid and s to the solid matrix. The thermal conductivity and the volumetric heat capacity are described in terms of a local volume average. Heat conductivity, density and heat capacity are assumed to be independent of temperature for simplicity and described by $\lambda = (1-\varphi)\lambda_s + \varphi\lambda_f$ and $\rho C = (1-\varphi)\rho_s C_s + \varphi\rho_w C_w$. This pore flow velocity can be determined for by using Darcy's formula for fluid flow through a porous medium:

$$q = \frac{k}{\mu} \nabla P \tag{6}$$

Where is k [m2] the intrinsic permeability, μ the constant viscosity of 0.001 Pa.s and P [Pa] the pressure. More detailed explanation about the modelling can be found in Saeid et al., (2014&2015).

3.3 NPV model

NPV of a geothermal doublet is determined utilizing the NPV model of Van Wees et al., (2010). The economic input parameters are listed in Table 2. NPV calculations are determined for a fifteen year period. This time period is chosen because it is the maximum duration of the Dutch feed-in tariff scheme (SDE+). 250.000 euro pump work-over costs are taken into account every five years, which is half of the estimated pump costs. The resulting NPV is equal to the depreciated, discounted, net-cumulative income after fifteen years.

Well costs per kilometer well length are presented Table 2. For simplification, it is assumed that a 2 km deep reservoir is reached in two stages, a 1km vertical and a deviated stage. The length of the wells is therefore approximated by the sum of the vertical stage (D_{vert}) and the deviated stage ($D_{deviated}$) which in turn is roughly equal to $\boldsymbol{D_{deviated}} = \sqrt{(\boldsymbol{TD} - \boldsymbol{D_{vert}})^2 + \left(\frac{1}{2}\boldsymbol{L}\right)^2}$. In this equation TD is the total well depth (2 km) and L the distance between the wells in the reservoir. For example, a reducing of the well spacing from 1000 m to 800, 600 and 400 m could therefore result in a reduction of the well length by 2, 3 and 5% respectively. The drilling costs reduce accordingly.

Table 2: Economic parameters for the NPV model based on Van Wees et al., (2010).

Economic parameters				
Heat price		€	6,00	EUR/ GJ
Electricity price for operations		€	22,22	EUR/ GJ
discount rate			7	%
Capex				
Well costs		*€*	*7,63*	*M€*
Pump		*€*	*0,50*	*M€*
Heat Exchanger		*€*	*0,10*	*M€*
Contingency costs (10%)		*€*	*0,89*	*M€*
SEI (insurance)		*€*	*0,69*	*M€*
Total Capex			9,69	M€
Opex			5	% of Capex/ y
Tax			25,5	% of taxable income
Depreciaton period			10	year
SDE+				
Base energy price (2015		€	0,052	EUR/ kWh
correction price (2015)		€	0,019	EUR/ kWh
contribution SDE+		€ 9,17		EUR/ GJ

1. RESULTS

4.1 NPV sensitivity analysis

The base case (BC) NPV is determined based on equation 1,2,3 and 4 and on the BC parameters in Figure 3. The BC well spacing is 1000m. In the sensitivity analysis, the parameters are divided into geological and production parameters. The range in geological parameters is derived from the WNB case study (section 2). The production parameters are varied by ±10% of the BC value. In the analysis, each parameter is varied individually while the others are kept at their BC value. The resulting change in NPV is presented in percentages in Figure 4. The results indicate that the most influential parameters are difference between injection and production temperature (ΔT) and flow rate. A 10% variation of these parameters could influence the NPV by approximately ± 40%. Furthermore, the results indicate that due to the geological uncertainties in reservoir thickness and average permeability in the WNB, the NPV could vary by approximately ±20%. Finally the results of this sensitivity analysis show that a 10% variation in well spacing (L) could result in a 10% variation in NPV.

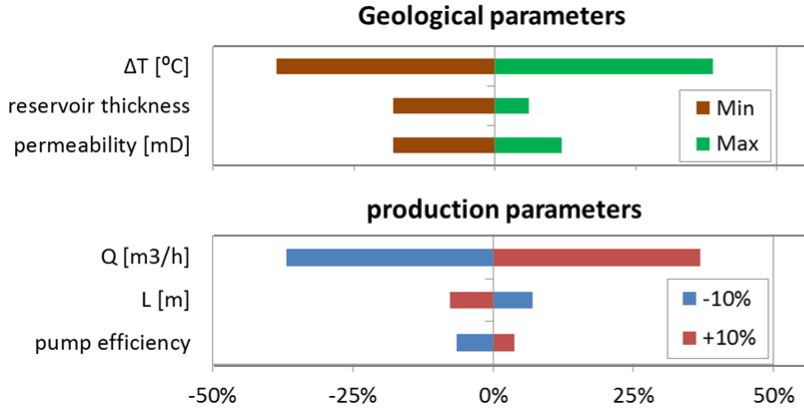

	Min	BC	Max
dT [°C]	36	40	44
reservoir height [m]	50	100	150
permeability [mD]	250	500	2000
	-10%	BC	10%
Q [m3/h]	90	100	165
L [m]	900	1000	1100
Pump efficiency	67,5%	75%	82,5%

Figure 3: NPV sensitivity analysis parameters are divided in 2 categories: geological and production related. The ranges of the parameters are shown in the table on the right. L is the well spacing. The resulting NPV variation is presented in percentages.

4.2 Detailed facies architecture production simulations

Some hundred-fifty production simulations are performed. In this simulations, thirteen detailed facies architecture models are used. N/G in these models varies from 15 to 70%. These simulations are compared to production simulations in homogeneous reservoir models. In this way the effect of facies architecture and the uncertainty in N/G is evaluated. Four well spacing distances and three different production flow rates are compared. In addition, two life time scenarios are used. In one scenario the doublet life time is reached when the production temperature dropped by 7.5°C which is equal to 10% of the initial reservoir temperature (henceforth scenario A). In the second scenario, the production temperature is only allowed to drop by 1 °C (henceforth scenario B). Figure 4 shows an overview of the results of $100m^3/h$ and $150m^3/h$ production simulations. The difference in life time between homogeneous and detailed facies architecture models shows the effect of facies architecture. The horizontal, black dotted lines indicate the minimal required fifteen year life time. In all well spacing and production rate scenarios, 400 m spacing is insufficient and hence not presented here. In the detailed architecture models, 600m spacing is only sufficient in life time scenario A. 800m spacing is sufficient in scenario B when the flow rate is $100m^3/h$. The result in Figure 4 indicate that due to uncertainty in N/G, the range in possible life time increases with increasing well spacing. Please note that the reservoir thickness in these results is only 50m. This is a very conservative value considering the thickness ranges described in section 2.

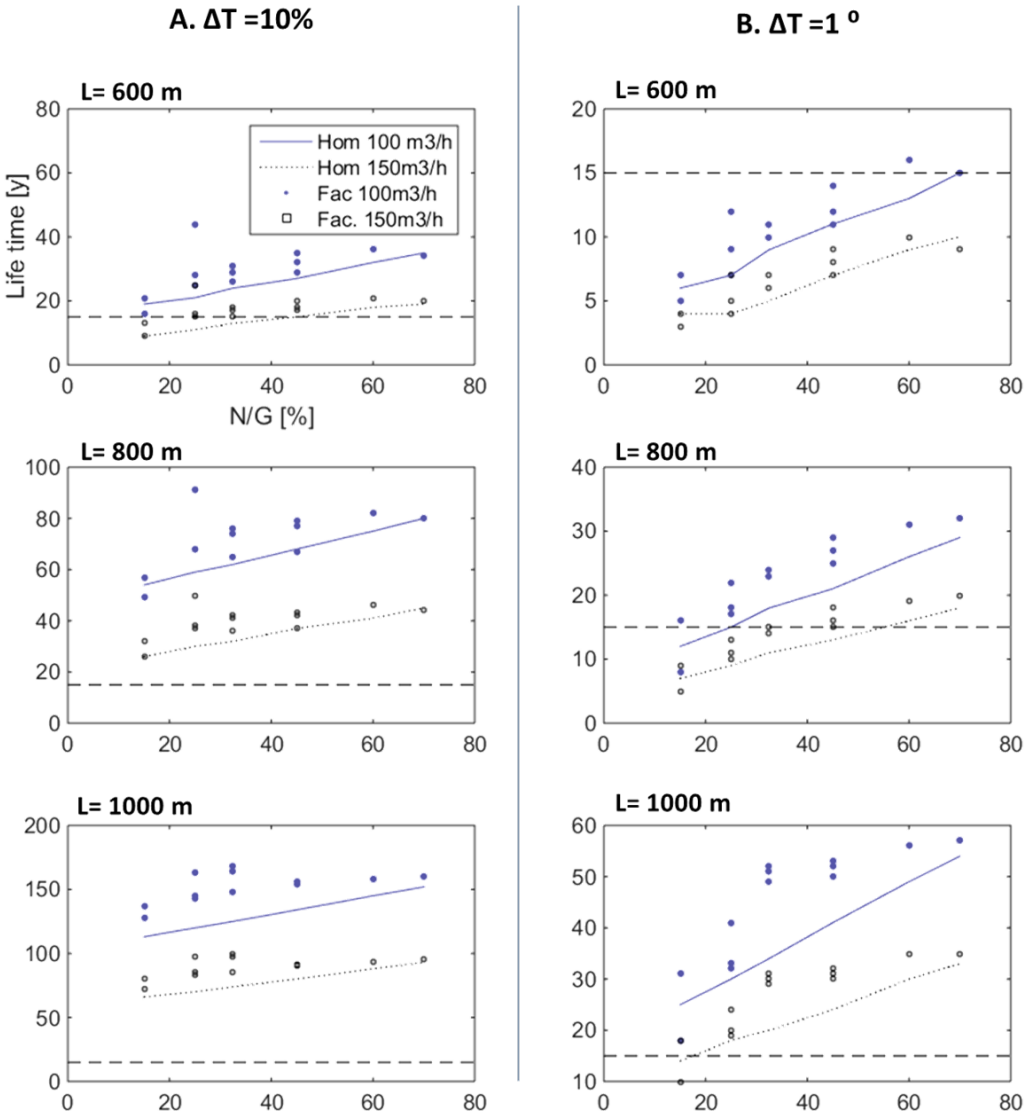

Figure 4: Life time ranges in the detailed facies architecture models in the two life time scenarios for 100 and 150 m^3/h flow rates. The column on the left presents results for life time scenario of a 10% production temperature drop (scenario A). The column on the right presents result of the life time scenario for a 1°C production temperature drop (scenario B).

Subsequently the production simulations are used to generate associated NPV to well spacing relations. This is presented in Figure 5-A. The NPV values from the thirteen detailed facies models are averaged. This average is compared to the NPV calculations for two homogeneous models of 15 and 70 % N/G. These results indicate that an optimum in NPV can be expected around 600m well spacing for the 70% N/G homogeneous model. If the reservoir volume decreases or if the life time uncertainty increases, this optimum shifts to a higher well spacing. In the case of the detailed facies architecture models and the low 15% N/G homogeneous model, this optimum in NPV is found around 800m. A reduction in well spacing also reduces the possible amount of recoverable heat from a doublet. Optimization of the amount of recoverable heat favors larger well spacing distance. Figure 5-B shows how the recoverable heat and NPV both relate to well spacing in a 50m thick homogeneous reservoir of 70% N/G at 100m^3/h production flow rate. Two optima are indicated. First, the optimal NPV at 600m spacing and second an optimum in both NPV and recoverable heat at approximately 900m spacing.

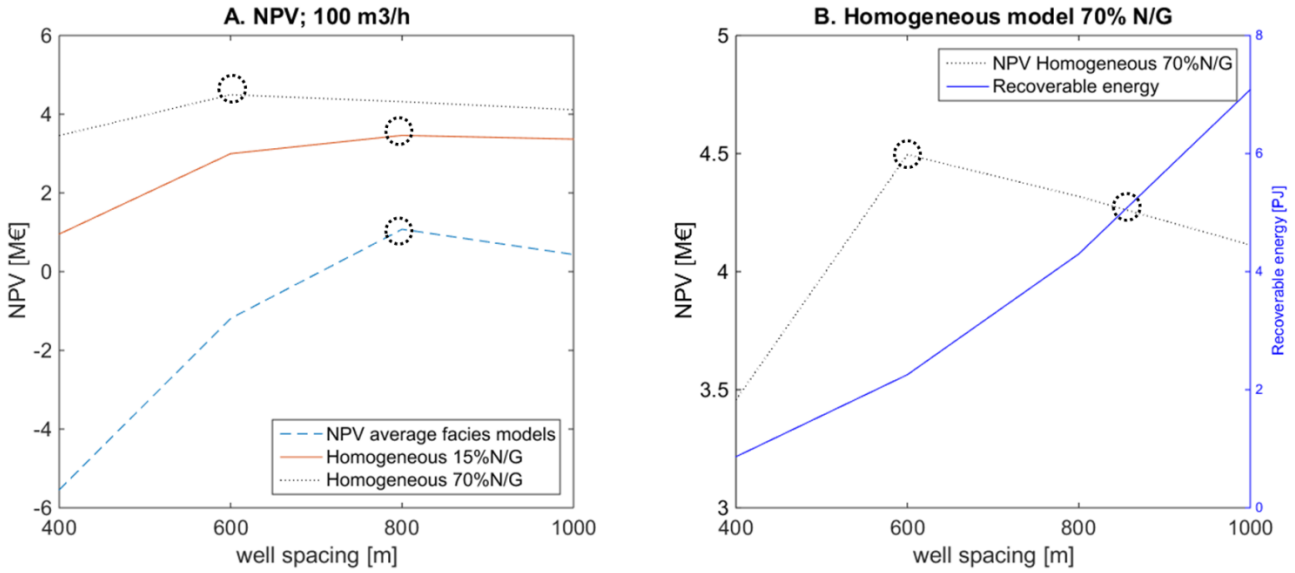

Figure 5: (A) Averaged NPV calculations for detailed facies architecture models compared to homogeneous reservoir models of 15 and 70% N/G with 100m^3/h production rate. Optima are indicated by the black dotted circles. (B) Comparison of NPV and the maximum recoverable energy for homogeneous 70% N/G model.

In Figure 6, the NPV is related to the capacity for all flow rate and N/G scenarios. Only the NPV and capacity in the 400 and 1000 m well spacing scenarios are presented. These results indicate how facies architecture and the uncertainty in N/G, results in an uncertainty in NPV and capacity. A minimal capacity of approximately 4MW is required for a positive NPV. This is only created in the higher N/G facies architecture models. Therefore, many of the lower N/G models have a negative NPV. The reservoir thickness used for these result is only 50m. This is a conservative estimate compared to the WNB examples. If reservoir models with a higher thickness would be used, the NPV vales would increases. In contrast the uncertainty in NPV and capacity would decrease. Finally a larger range in NPV is recognized in the doublets with a 1000m spacing. This is a result of the larger spread in life time associated with larger well spacing.

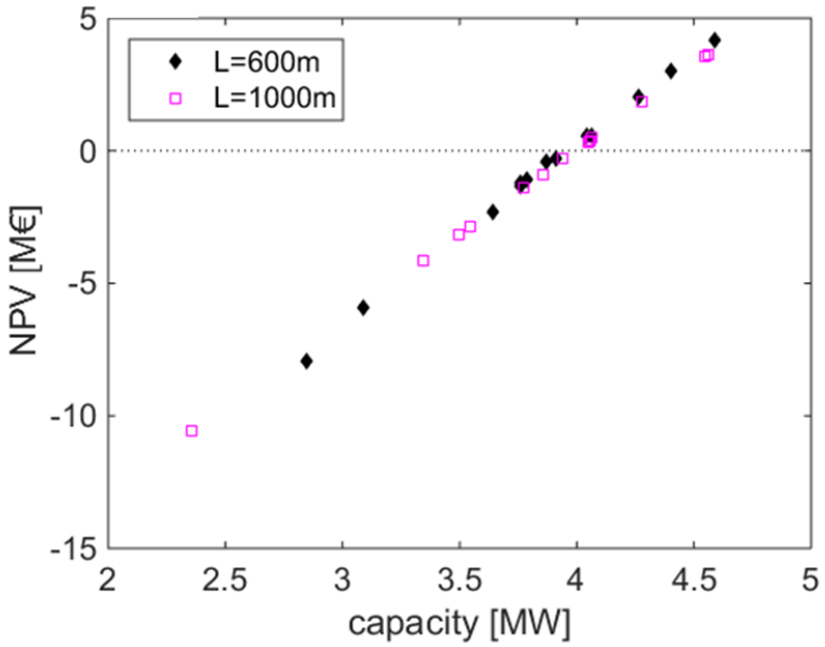

Figure 6: NPV relation to doublet capacity of detailed facies architecture models with 600 and 1000m well spacing. The horizontal line indicates the zero NPV threshold.

CONCLUSION

In this paper, the relation between well spacing and Net Present Value of a HSA geothermal doublet is analyzed. Parameters in this analysis are derived from a WNB case study. The study is divided into two parts. First, a sensitivity analysis is carried out to compare the effects of variation of geological and production parameters on the doublet NPV. This analysis shows that the reservoir temperature and flow rate are the most influential of the parameters considered in this study. A 10% variation could lead to approximately 40% variation in NPV. The geological uncertainty in permeability and reservoir thickness, that result from the WNB subsurface data analysis, can account for a 20% variation in NPV. Third, a 10% variation in well spacing could lead to a 10% variation in NPV. When the life time is lower than 15 years, NPV drops rapidly with decreasing well spacing. A disadvantage of a reduction in well spacing is the reduction of the amount of possible recoverable energy from the doublet. Further, to see the effect of reservoir architecture on doublet capacity and life time, finite element production simulations are carried out in reservoir models which are generated utilizing a process-based facies modelling approach. Our results highlight the importance of taking fluvial reservoir architecture into account in the assessment of the potential of HSA doublets.

REFERENCES

Bonté, D., Van Wees, J.D., Verweij, J.M. : Subsurface temperature of the onshore Netherlands: new temperature dataset and modelling, *Netherlands Journal of Geosciences,* **91(4)**, (2012), 491-515.

Boxem, T.A.P., Van Wees, J.D., Plauymaekers, M.P.D., Beekman, Batini,, F., Bruhn, D.F., Calcagno, Manzella, A., Schellschmidt : ThermoGIS World Aquifer Viewer - An Interactive Geothermal Aquifer Resource Assessment Web-tool. *1st EAGE Sustainable Earth Sciences Conference and Exhibition*. (2011). DOI: 10.3997/2214-4609.20144176.

Cojan, I., Fouche, O. & Lopez, S.: Process-based reservoir modelling in the example meandering channel. In: *Leuangthong, O. & Deutsch, C. (eds) Geostatistics Banff 2004*. Springer, Dordrecht, (2004), 611–619.

Donselaar, M.E., Overeem, I.: Connectivity of fluvial point-bar deposits: An example from the Miocene Huesca fluvial fan, Ebro Basin, Spain. *AAPG Bulletin*, **92(9),** (2008), 1109-1129.

Gibling, M.R..: Width and thickness of fluvial channel bodies and valley fills in the geological record: A literature compilation and classification. *Journal of Sedimentary Research*, **76**, (2006), 731-770. DOI: 10.2110/jsr.2006.060.

Gonzales, L. Aardwarmte, De duurzaamheid van Geothermie. (2013). *Rapportage Platform Geothermie.*

Grappe B., Cojan I., Flipo N., Rivoirard J., Vilmin L.: Developments in Dynamic Modelling of Meandering Fluvial Systems. *AAPG 2012* congress, (2012).

Gringarten, A.C.,: Reservoir Lifetime and Heat-Recovery factor in Geothermal Aquifers used for Urban Heating. *Pure and Applied Geophysics*, **117**, (1978), 297-308, ISSN: 0033-4553

Hamm, V., Lopez, S.: Impact of Fluvial Sedimentary Heterogeneities on Heat Transfer at a Geothermal Doublet Scale. *Stanford Geothermal Workshop*, Jan 2012, Stanford, United States. SGP-TR-194, (2012), p. 18.

Larue, D.K., Friedmann, F.: The controversy concerning stratigraphic architecture of channelized reservoirs and recovery by waterflooding. Petroleum Geoscience, **11**, (2005), 131-146.

Larue, D.K., Hovadik , J.M.: Connectivity of Channelized reservoirs: a modelling approach: *Petroleum Geology*, **12**, (2006), 291-308, doi: 10.1144/1354-079306-699.

Larue, D.K., Hovadik, J.: Why is reservoir architecture an insignificant uncertainty in many appraisal and development studies of clastic channelized reservoirs? *Journal of Pertroleum Geology*, **31 (4)**, (2008), 337-366.

Lopez, S., Cojan, I., Rivoirard, J., and Galli, A.: Process-based stochastic modelling: meandering channelized reservoirs. Analogue Numer Model Sediment Syst: 616 From Understand Predict. *Special Publ. **40** of the IAS*, (2009).

Lopez, S., Hamm, H., Le Brun, M., Schaper, L., Boissier, Cotiche, C., Gioglaris, E.: 40 years of Dogger aquifer management in Ile-de-France, Paris Basin, France. *Geothermics*, ., (2010), 39, 339-356.

Mijnlieff, H., Van Wees, J.D.: Rapportage Ruimtelijke Ordening Geothermie, *TNO report*, (2007)..

Mottaghy, D., Pechig, R., Vogt., C.: The geothermal project Den Haag: 3D numerical models for temperature prediction and reservoir simulation. *Geothermics*, **40**, (2011). 199-210.

Poulsen, S.E., Balling, N., Nielsen, S.B.: A parametric study of the thermal recharge of low enthalpy geothermal reservoirs. *Geothermics,* **53**, (2015), 464-478.

Pranter, M.J., Sommer, N.K.: Static connectivity of fluvial sandstones in a lower coastal-plain setting: An example from the Upper Cretaceous lower Williams Fork Formation, Piceance Basin, Colorado.*AAPG Bulletin*, **95 (6)**, (2011), 899-923.

Pujol, M., Richard, L.P., Bolton, G.: 20 years of exploitation of the Yarragadee aquifer in the Perth Basin of Western Australia for direct-use of geothermal heat. *Geothermics*, **57**, (2015), 39-55.

Saeid, S., Al-Khoury, R., Nick, H. M., & Barends, F.: Experimental–numerical study of heat flow in deep low-enthalpy geothermal conditions. *Renewable Energy*, **62**, (2014), 716-730.

Saeid, S., Al-Khoury, R., Nick, H.M., Hicks, M.A.: A prototype design model for deep low-enthalpy hydrothermal systems. *Renewable Energy*, **77**, (2015), 408-422.

TNO Nl olie- en gasportaal, www.nlog.nl, (1977).

Van Heekeren, V., Bakema, G.: The Netherlands Country Update on Geothermal Energy. *European Geothermal Congress 2013* Pisa (2013), Italy.

Van Heekeren, V., Bakema, G.: The Netherlands Country Update on Geothermal Energy. *Proceedings World Geothermal Congress 2015*, (2015).

Van Wees J.D.A.M, Kramers, I., Kronimus, R.A., Pluymaekers., M.P.D, Mijnlieff, H.F and Vis, G.J.: "ThermoGis V1.0, Part II: Methodology", *TNO-Report,* (2010).

Van Wees, J.D.A.M., Konimus, A., van Putten, M., Pluymaekers, M.P.D., Mijnlieff, H., van Hooff, P., Obdam, A. & Kramers,L.: Geothermal aquifer performance assessment for direct heat production – Methodology and application to Rotliegend aquifers. *TNO Report,* (2012).

Villamizar, C.A., Hampson., G.J., Flood, Y.S., Fitch, P.J.R.: Object-based modelling of avulsion-generated sandbody distributions and connectivity in a fluvial reservoir analogue of low to moderate net-to-gross ratio. *Petroleum Geoscience*, **21**, (2015), 249-270. doi:10.1144/petgeo2015-004.

Willis, B.J., Tang, H.: Three-Dimensional Connectivity of Point-Bar Deposits. *Journal of Sedimentary Research*, **80 (5),** (2010), 440-454. doi: 10.2110/jsr.2010.046.